J Solid State Electrochem (2010) 14:1929–1936
DOI 10.1007/s10008-010-1034-8

ORIGINAL PAPER

Adsorption and redox chemistry of *cis*-RuLL'$(SCN)_2$ with L=4,4′-dicarboxylic acid-2,2′-bipyridine and L'=4,4′-dinonyl-2,2′-bipyridine (Z907) at FTO and TiO_2 electrode surfaces

Alberto Fattori · Laurence M. Peter · Keri L. McCall · Neil Robertson · Frank Marken

Received: 13 January 2010 / Revised: 9 February 2010 / Accepted: 10 February 2010 / Published online: 16 March 2010

Abstract The electrochemical and spectroelectrochemical properties of the sensitizer dye Z907 (*cis*-RuLL'$(SCN)_2$ with L=4,4′-dicarboxylic acid-2,2′-bipyridine and L'=4,4′-dinonyl-2,2′-bipyridine) adsorbed on fluorine-doped tin oxide (FTO) and TiO_2 surfaces have been investigated. Langmuirian binding constants for FTO and TiO_2 are estimated to be 3×10^6 M^{-1} and 4×10^4 M^{-1}, respectively. The Ru(III/II) redox process is monitored by voltammetry and by spectroelectrochemistry. For Z907 adsorbed onto FTO, a slow EC-type electrochemical reaction is observed with a chemical rate constant of ca. $k=10^{-2}$ s^{-1} leading to Z907 dye degradation of a fraction of the FTO-adsorbed dye. The Z907 adsorption conditions affect the degradation process. No significant degradation was observed for TiO_2-adsorbed dye. Degradation of the Z907 dye affects the electron hopping conduction at the FTO–TiO_2 interface.

Keywords Solar cell · Sensitizer · Dye · TiO_2 · FTO · Voltammetry · Mechanism · Conduction · Semiconductor

Introduction

The need for renewable sources of cheap and sustainable energy presents an important challenge. Photovoltaic devices are now becoming competitive for low-cost large-scale manufacturing as efficiency and durability of devices is further improved. Dye sensitised solar cells (DSCs), proposed by Grätzel in 1991 [1, 2], generate electrical power by mimicking the natural photosynthesis process. Key components of a DSC are a sensitizer (dye), a mesoporous semiconductor and electrolyte. The dye harvests light in the visible range and it injects electrons into the semiconductor (usually TiO_2) conduction band. The oxidised dye is then regenerated by electron donation from the electrolyte, which usually contains the iodide/triiodide redox couple [3, 4]. The efficiency of DSCs can be improved by optimising the physical and chemical properties of these components [5]. The understanding of the redox properties and chemical stability of the oxidised form of the dye is of crucial importance for the optimization of long-lived DSCs. The most successful sensitizer dyes for DSCs are poly-pyridyl ruthenium complexes [6, 7].

In order to guarantee a long lifetime of a DSC, the dye should be able to undergo millions of redox cycles before degradation occurs. Important parameters that influence the long-term stability of a DSC are the ability of a dye to survive elevated temperatures and to exhibit a sufficiently stable Ru(III) oxidised form. Dyes like *cis*-RuLL'$(SCN)_2$ with L=4,4′-dicarboxylic acid-2,2′-bipyridine and L'=4,4′-dinonyl-2,2′-bipyridine (also known has Z907; see Fig. 1) are reported to fulfil these requirements [8, 9]. One very successful approach for avoiding the photochemical degradation of dye systems has been to alter the ligand structure. In the dye Z907, one bipyridyl ligand has been modified by attaching two nonyl hydrocarbon chains [8]. This modification has been reported to significantly enhance the chemical stability in the oxidised form, and no direct observation of chemical degradation processes have been reported to date.

A. Fattori · L. M. Peter · F. Marken (✉)
Department of Chemistry, University of Bath,
Claverton Down,
Bath BA2 7AY, UK
e-mail: F.Marken@bath.ac.uk

K. L. McCall · N. Robertson
School of Chemistry, University of Edinburgh,
King's Buildings, West Mains Road,
Edinburgh, Scotland EH9 3JJ

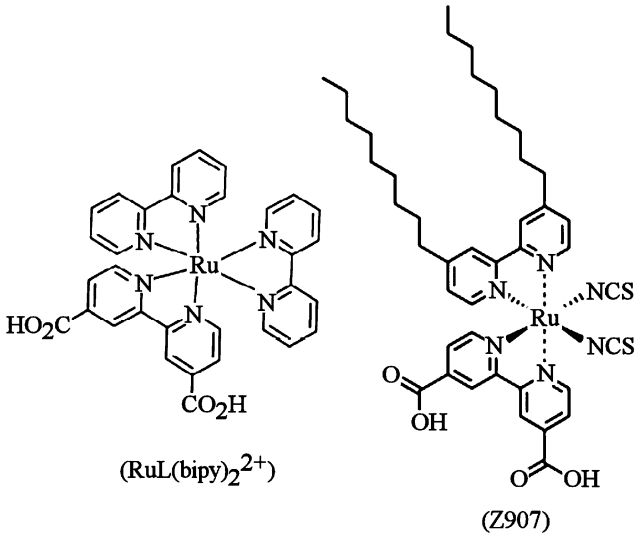

Fig. 1 Molecular structures for $RuL(bipy)_2^{2+}$ and for Z907 (*cis*-$RuLL'(SCN)_2$ with L=4,4′-dicarboxylic acid-2,2′-bipyridine and L'=4,4′-dinonyl-2,2′-bipyridine)

The way in which the sensitizer is attached to the semiconductor surface may affect reactivity and the electron injection kinetics [10]. In order for the dye to attach to the TiO_2 semiconductor substrate, functional groups such as carboxylate are required to form a strong bond [11]. Grätzel and coworkers [12] have reported that for three polypyridyl ruthenium dyes (including Z907) attached on TiO_2, charge transport may occur via Ru(III/II) electron hopping. This mechanism is effective if there is good electronic interaction associated with close packing of the dye molecules on the oxide surface. Typical electron diffusion coefficients are 10^{-13} m^2 s^{-1}. Although this Ru(III/II) charge hopping process may be of only secondary importance for solar cell operation, it could lead to electron/Ru(III) recombination at the fluorine-doped tin oxide (FTO) back electrode.

Previous studies on the DSC sensitizer *cis*-bis(isothiocyanato)-bis(2,2′-bipyridyl-4,4′ dicarboxylato)-ruthenium (II) (or N719) have shown that electron hopping between adsorbed dye molecules is strongly affected by the chemical degradation of the oxidised sensitizer. The study of N719 adsorbed at the surface of FTO and FTO–TiO_2 electrodes immersed in acetonitrile electrolyte revealed EC-type degradation with k=2.4 s^{-1} [13]. N719 is a highly successful dye because the degradation process is many orders of magnitude slower than regeneration by electron transfer from iodide. Degradation predominantly affects FTO-adsorbed dye, and this could even result in a beneficial effect since it retards electron/Ru(III) recombination at the FTO–TiO_2 interface by suppressing electron hopping.

In the present study, surface redox processes were investigated first for a fully chemically reversible surface redox system—$RuL(bipy)_2^{2+}$ (with L=4,4′-dicarboxylic acid-2,2′-bipyridine)—and then for the more reactive Z907 redox system (see Fig. 1). Cyclic voltammetry revealed that the dye adsorption conditions influence the chemical stability of Z907 film. The degradation rate for the oxidised Z907 adsorbed on FTO was found to be approximately two orders of magnitude slower compared to that determined previously for the oxidised N719 [13].

Experimental details

Chemical reagents

Acetonitrile (HPLC grade) was obtained from Fisher Scientific. Tetrabutylammonium hexafluorophosphate (NBu_4PF_6, electrochemical grade), tetrabutylammonium iodide (puriss.) and tert.-butanol (ACS>99.7% GC) were purchased from Fluka. LiI (anhydrous 99.99%) was obtained from Aldrich. The dye Z907 *cis*-bis(isothiocyanato)-(2,2′-bipyridyl-4,4′-dicarboxylic acid)-(2,2′-bipyridyl-4,4′-dinonyl)-ruthenium(II) and TiO_2 HT colloid (9 nm average particle diameter) were purchased from Solaronix. The metal complex $RuL(bipy)_2^{2+}$ with L=4,4′-dicarboxylic acid-2,2′-bipyridine was prepared following a literature procedure [14]. Sodium hydroxide (Sigma ultra minimum 98%) was obtained from Sigma-Aldrich. Ethanol (absolute) was purchased from Fisher Scientific.

Instrumentation

An Autolab potentiostat (PGSTAT 12, Ecochemie, the Netherlands) was employed for all voltammetric studies. A Pt foil counter electrode with a surface area of 30 mm^2 was employed for electrochemical studies and a Pt wire was employed for spectroelectrochemical studies. For spectroelectrochemical studies a potentiostat from Ivium Technologies (Compactstat electrochemical interface) was employed. The working electrode was a FTO-coated glass from Asahi Glass Fabritech (AGC type U TCO glass, Japan). For the electrochemical studies the active exposed surface area for the FTO and FTO–TiO_2 electrodes was either 42 or 9 mm^2 and for spectroelectrochemical studies for FTO–TiO_2 the area was 16.8 mm^2. The reference electrode employed was Ag/AgCl (3 M KCl) from CH Instruments Incorporated. Experiments were conducted after thorough de-aerating with argon for at least 15 min. The temperature during the experiments was 20±2 °C. UV/Vis spectroscopy and spectroelectrochemical studies were carried out with Varian Cary 50 UV-Vis spectrophotometer.

Preparation of FTO-TiO_2 film electrodes

FTO slides were washed and sonicated five times for 15 min each in water, ethanol, twice in isopropanol and

finally analytical grade ethanol. In order to reduce series resistance losses, a gold stripe was evaporated onto FTO electrode surface (not exposed to the solution). FTO–TiO_2 films were prepared by "doctor blading" (uniformly spreading TiO_2 paste on a pre-defined area of FTO glass with a glass bar). The FTO electrode was then left for 30 min on a hot plate at 450 °C in order to sinter the anatase crystals. Z907 dye adsorption on bare FTO or on FTO–TiO_2 film electrodes was carried out by heating the electrodes for 30 min at 450 °C on a hot plate, cooling down to 75 °C and immersion into a solution of Z907 dye in 50% acetonitrile 50% *tert.*-BuOH for a given time (typically with 10^{-4} M Z907 dye in 50% acetonitrile 50% *tert.*-BuOH for a period of 16 h).

Results and discussion

Adsorption and redox chemistry of $RuL(bipy)_2^{2+}$ with L=4,4′-dicarboxylic acid-2,2′-bipyridine at FTO thin film electrode surfaces

A chemically stable model redox system, $RuL(bipy)_2^{2+}$ with L=4,4′-dicarboxylic acid-2,2′-bipyridine was employed initially to demonstrate well-defined redox processes at FTO film electrodes without the complication of additional chemical follow-up processes. Adsorbed monolayers of the Ru(III/II) system $RuL(bipy)_2^{2+}$ at FTO surfaces have been studied previously for application in electroluminescence analysis, and stable redox chemistry in aqueous media was reported [15].

Figure 2a shows cyclic voltammograms for the oxidation of $RuL(bipy)_2^{2+}$ adsorbed onto FTO. The reversible potential for the Ru(III/II) process is ca. 1.34 V versus Ag/AgCl(3 M KCl). A plot of the oxidation peak current versus scan rate (see Fig. 2b) is linear and consistent with a surface-immobilised redox system. Analysis of the charge under the cyclic voltammetric response, corresponding to 4.4 μC cm^{-2}, can be compared with the theoretical value for monolayer adsorption. Taking an area of ca. 2 nm^2 occupied by each $RuL(bipy)_2^{2+}$ [16], and a roughness factor of 1.5, the theoretical monolayer coverage is estimated as 12 μC cm^{-2}, which suggests that close packing is not achieved experimentally. The peak width at half height for the voltammetric signal is approximately 110 mV compared to the ideal theoretical value of 91 mV at 25 °C [17]. The peak-to-peak separation for the cyclic voltammograms shown in Fig. 2a are most likely indicative of a slow interfacial electron transfer. The voltammetric responses remained unchanged over many experiments and therefore demonstrate the chemical inertness of the $RuL(bipy)_2^{2+}$ redox system. Next, the electrochemical characteristics are compared to Z907 adsorbed onto FTO electrodes.

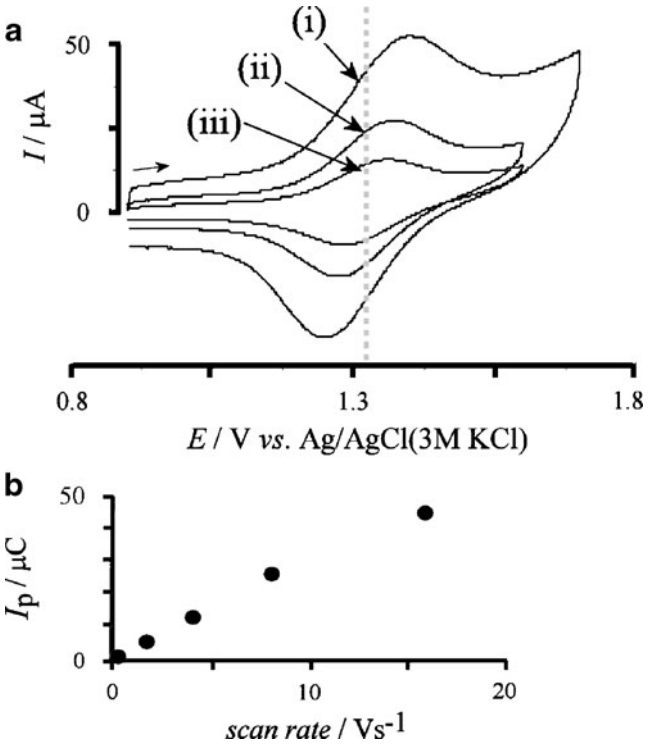

Fig. 2 **a** Cyclic voltammograms (scan rate (*i*) 16, (*ii*) 8 and (*iii*) 4 V s^{-1}) for the oxidation and back reduction of $RuL(bipy)_2^{2+}$ (with L=4,4′-dicarboxylic acid-2,2′-bipyridine) adsorbed onto a 9-mm^2 FTO electrode (1 h in 10^{-5} M dye solution) and immersed in acetonitrile/0.1 M NBu_4PF_6. **b** Plot of the peak current for the oxidation peak versus scan rate

Adsorption and redox chemistry of cis-$RuLL'(SCN)_2$ with L=4,4′-dicarboxylic acid-2,2′-bipyridine and L'=4,4′-dinonyl-2,2′-bipyridine (Z907) at FTO thin film electrode surfaces

The Z907 sensitizer dye (see Fig. 1) has been thoroughly studied [18] and employed in solar cell devices. However, there is no previous study of the chemical reactivity of Z907 immobilised by adsorption onto FTO, which is commonly employed as a substrate in solar cell assemblies. The voltammograms shown in Fig. 3a demonstrate the facile adsorption of Z907 onto FTO surfaces and the resulting well-defined oxidation and reduction processes with a reversible potential of ca. 0.68 V versus Ag/AgCl (3 M KCl). The charge under the oxidation peak is approximately 11 μC cm^{-2} which is in excellent agreement with the theoretical prediction (vide supra). A plot of the charge under the oxidation peak versus the Z907 concentration during the adsorption process shows Langmuirian characteristics (see Fig. 3c) with an estimated binding constant of $K=3\times10^6$ M^{-1}.

The shape of the voltammetric responses is broad (width at half height approximately 250 mV) indicating either different types of binding sites, intermolecular interactions

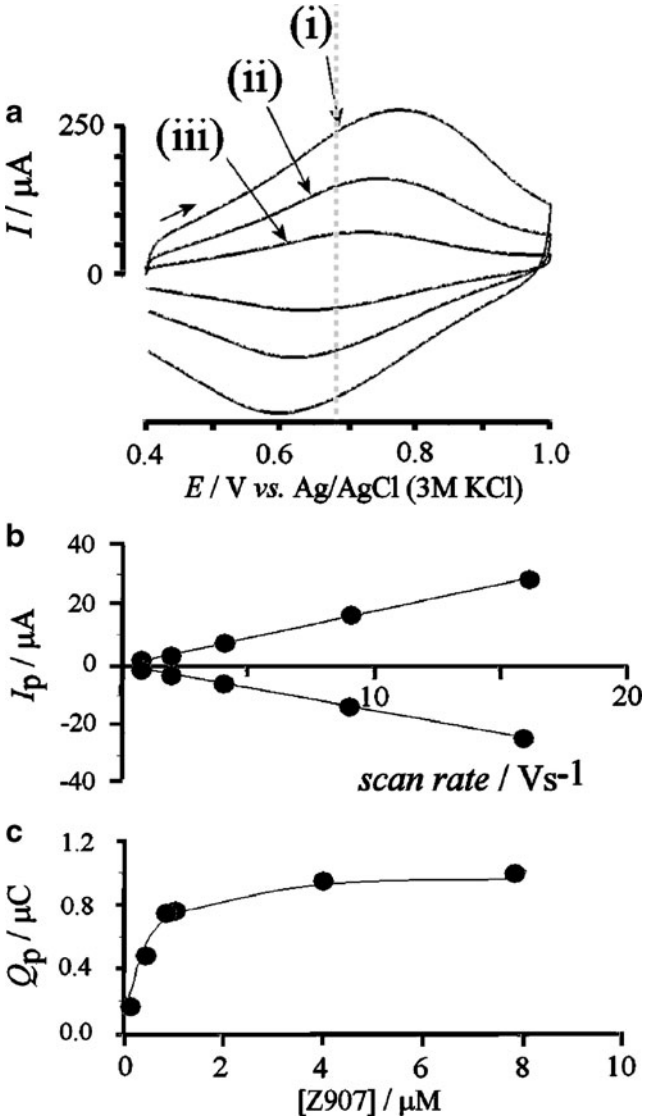

Fig. 3 **a** Cyclic voltammograms (scan rate (*i*) 16, (*ii*) 8 and (*iii*) 4 V s^{-1}) for the oxidation and back reduction for Z907 adsorbed on a 42-mm^2 FTO electrode (1 h in 10^{-6} M dye solution) and immersed in acetonitrile/0.1 M NBu_4PF_6. **b** Plot of the peak currents versus scan rate. **c** Plot of the charge under the oxidation peak (scan rate 16 V s^{-1}) versus concentration of Z907 in the dye solution. The *line* corresponds to a Langmuirian binding constant of $K=3\times10^6$ M^{-1}. The electrodes used in this experiment had an active surface area of 9 mm^2

or different binding modes (orientations). The peak-to-peak separation of the cyclic voltammograms in Fig. 3a appears very similar to that in Fig. 2a and is therefore again attributed predominantly to slow electron transfer kinetics. The peak-to-peak separation of ca. $\Delta E_p=180$ mV at a scan rate of $v=16$ V s^{-1} can be used to estimate the standard rate constant for interfacial electron transfer, $k_e\approx2\times10^3$ s^{-1}, based on the expression $\frac{\Delta E_p}{2}=\frac{RT}{\alpha F}\ln\left(\frac{RTk_e}{\alpha Fv}\right)$ with $\alpha=1/2$ assumed [19].

Closer inspection of the voltammetric data obtained at slower scan rates reveals a loss of charge sequentially cycle-by-cycle (see Fig. 4a). The fast cyclic voltammo-

Fig. 4 **a** Cyclic voltammograms (scan rate 16 V s^{-1}) for the oxidation and back reduction of Z907 adsorbed onto a 9-mm^2 FTO electrode (1 h in 10^{-6} M dye solution) and immersed in acetonitrile/0.1 M NBu_4PF_6. The three cyclic voltammograms represent (*i*) the first potential cycle, (*ii*) the potential cycle recorded after a slow potential cycle at 10 mV s^{-1} (not shown) and (*iii*) the potential cycle after a further slow potential cycle (not shown). **b** Plot of the charge under the oxidation peak, Q_p (recorded at 16 V s^{-1}), versus the number of slow potential cycles (10 mV s^{-1}) for Z907 adsorbed onto FTO (1 h in a 10^{-6} M dye solution). The *line* shows a theoretical decay for a chemical rate constant $k=1.1\times10^{-2}$ s^{-1}. Electrode area was 9 mm^2. **c** As before (1 h in a 0.5×10^{-3} M dye solution). The *line* shows a theoretical decay for a chemical rate constant $k=8\times10^{-3}$ s^{-1}. Electrode area was 9 mm^2 (**d**) as before (16 h in a 0.5×10^{-3} M dye solution). The *line* shows a theoretical decay for a chemical rate constant $k=5\times10^{-3}$ s^{-1}. Electrode area was 9 mm^2. **e** Schematic drawing of the orientation of immobilised Z907 dye molecules at the FTO electrode surface and possible nucleophilic attack (see text)

grams (scan rate 16 V s^{-1}) was used as a probe measurement, and a slow cyclic voltammograms (not shown, scan rate 10 mV s^{-1}) was employed to enhance the loss effects which are attributed here to a chemical degradation process similar to that observed for the structurally related N719 dye [14]. The alternative mechanism of a loss of Z907 caused by simple desorption cannot be entirely ruled out but appears less likely (vide infra). The chemical degradation of Z907 was followed as a function of the number of slow potential cycles (see Fig. 4b–d). Interestingly, the loss of the Z907 response caused by slow scan rate experiments was found to depend on the conditions during the adsorption process. Data in Fig. 4b–d have been obtained for two different Z907 concentrations and for two different equilibration times. In order to analyse these "decay curves", first order decay kinetics has been assumed with only a fraction of the adsorbed Z907 chemically reactive. In particular, for higher Z907 concentrations and for extended equilibration times a fraction of the Z907 complex appeared to be inert. The expression for fitting the decay curves (see Fig. 4b–d) has therefore two terms for (a) inert Z907 with a surface concentration $\left[Z_0^{\text{inert}}\right]$ and (b) reactive Z907 with an initial surface concentration $\left[Z_0^{\text{reactive}}\right]$ (see Eq. 1).

$$[Z(t)]=\left[Z_0^{\text{inert}}\right]+\left[Z_0^{\text{reactive}}\right]e^{-kt_{ox}} \quad (1)$$

In this expression the chemical rate constant k can be obtained when the oxidation time (the time during slow scan cyclic voltammograms with applied potential positive of the reversible Ru(III/II) potential) is estimated (here $t_{ox}=112$ s). The surface concentration of Z907 is expressed in terms of the charge under the oxidation response. Figure 4b shows the data obtained for Z907 adsorption for 1 h from a 10^{-6} M solution. The fraction of reactive Z907 is estimated to be 90%, and the decay rate constant $k=1.1\times10^{-2}$ s^{-1}. In contrast, in Fig. 4c (adsorption for 1 h from 0.5×10^{-3} M

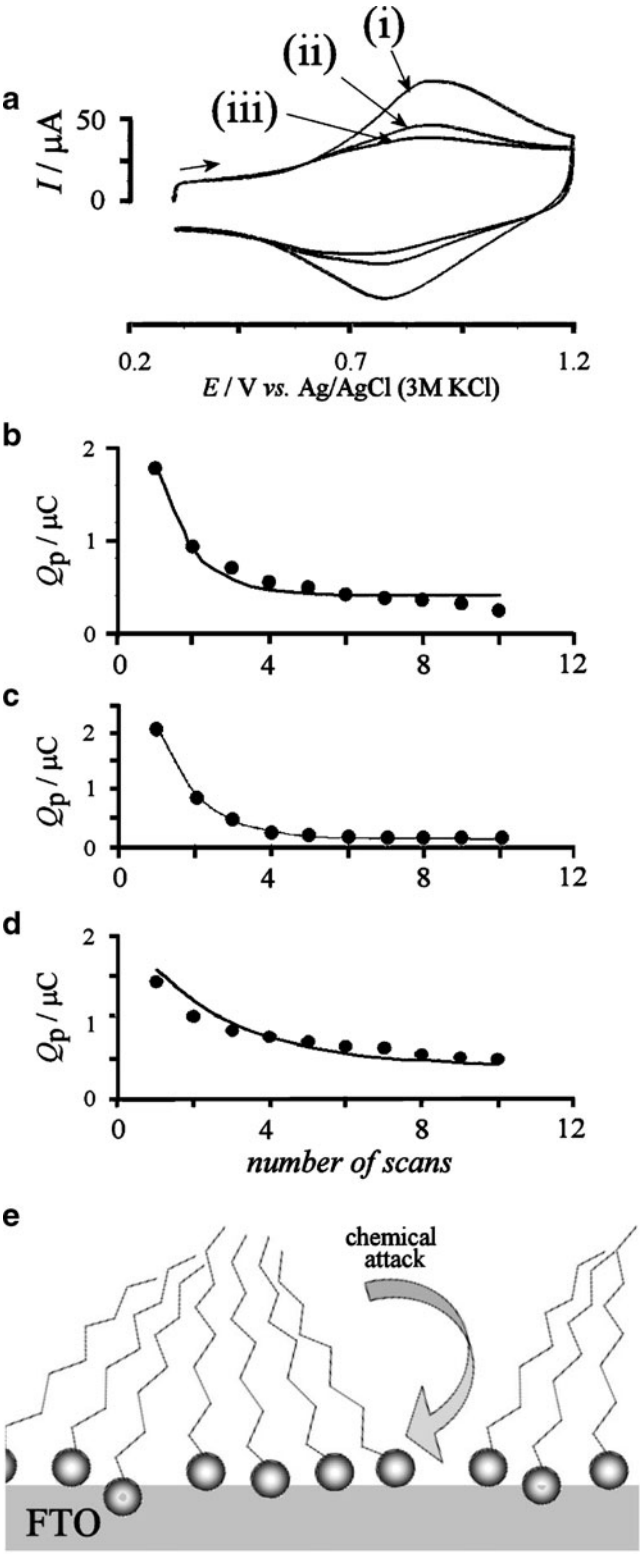

solution) the fraction of reactive Z907 is 98% and the decay rate constant $k=0.8\times10^{-2}$ s^{-1}. Finally, in Fig. 4d (adsorption for 16 h from 0.5×10^{-3} M solution) the fraction of reactive Z907 is 82% and the decay rate constant $k=0.5\times10^{-2}$ s^{-1}. Although the variation in the rate constant is small, there is a clear trend of slower decay with higher Z907 concentration and with a prolonged adsorption time. More importantly, the fraction of inert Z907 on the electrode surface can be increased by a longer adsorption period and this impacts on the initial rate of decay (see Fig. 4d).

The decay rate constant for Z907, $k=0.5\times10^{-2}$ s^{-1}, is more than two orders of magnitude slower compared to the

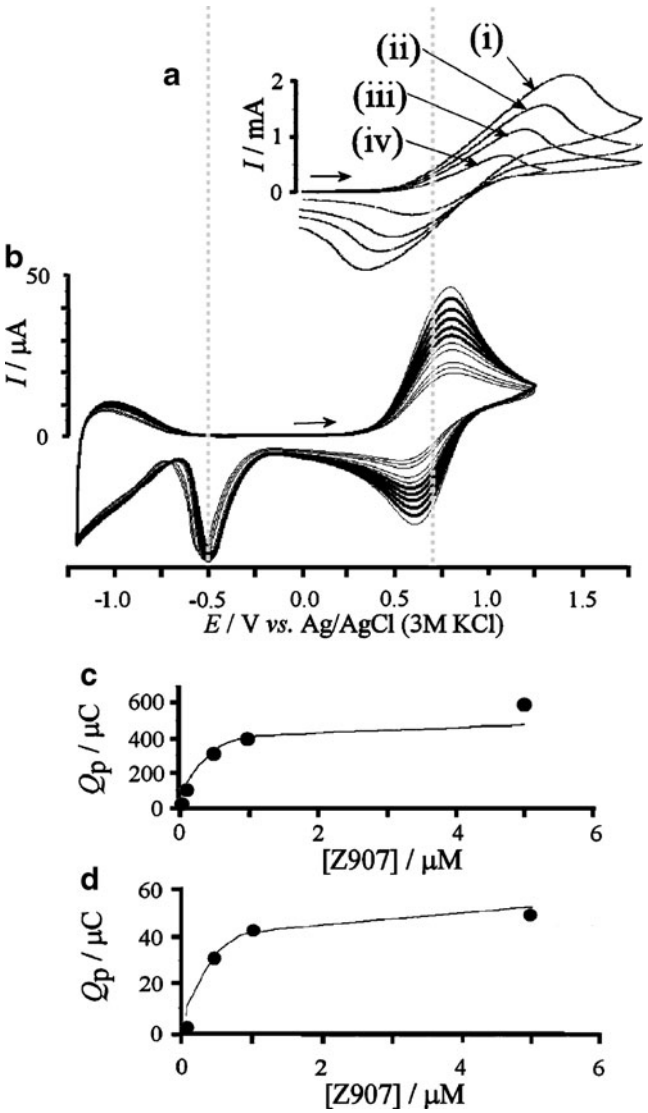

Fig. 5 **a** Cyclic voltammetry (scan rates (*i*) 16, (*ii*) 8, (*iii*) 4 and (*iv*) 1.6 V s^{-1}) for the oxidation and back reduction of Z907 adsorbed onto a FTO–TiO_2 film electrode (16 h in 10^{-4} M dye solution) immersed in acetonitrile/0.1 M NBu_4PF_6. **b** Multi-scan cyclic voltammetry (scan rate 0.1 V s^{-1}) for the oxidation and re-reduction of Z907 adsorbed onto a FTO–TiO_2 film electrode (16 h in 10^{-4} M dye solution) immersed in acetonitrile/0.1 NBu_4PF_6. **c** Plot of the charge under the oxidation peak versus concentration of Z907 during dye adsorption (16 h in dye solution). *Scan rate* is 16 mV s^{-1}. The *line* corresponds to a Langmuirian binding constant $K=4\times10^4$ M^{-1}. **d** As before but with a scan rate of 16 Vs^{-1}. The *line* corresponds to a Langmuirian binding constant $K=4\times10^4$ M^{-1}

value [13] of k=2.4 s^{-1} observed for the related dye N719 (which has the same molecular structure, but without nonyl functionalities). For structurally closely related Ru complexes a degradation reaction via ligand loss has been proposed [20]. The retardation of the degradation process is likely to arise from the steric hindrance effect introduced by the packing of nonyl functionalities. The decrease in reactivity when a longer period of adsorption is employed is consistent with improved ordering of the adsorbed Z907 on the FTO electrode surface. Figure 4e summarises the idea of ordering and steric shielding.

Adsorption and redox chemistry of cis-RuLL'$(SCN)_2$ with L=4,4′-dicarboxylic acid-2,2′-bipyridine and L'=4,4′-dinonyl-2,2′-bipyridine (Z907) at FTO-TiO_2 thin film electrode surfaces

Z907 was adsorbed onto FTO–TiO_2 electrodes with a thin mesoporous TiO_2 film of approximately 3 μm thickness. The cyclic voltammograms shown in Fig. 5a show a substantial increase in current and in the charge under the voltammetric response in the presence of the TiO_2. The peak current at fast scan rate (16 V s^{-1}) is increased by a factor ten (see Figs. 3a and 5a), and the charge under the oxidation process can reach 600 μC (compared to ca. 1 μC for bare FTO). Due to slow electron diffusion within the film, a slow scan rate was required in order to determine the overall charge. Typical apparent diffusion coefficients for charge hopping are reported to be $D \approx 10^{-13}$ m^2 s^{-1},[12] which leads to an estimated diffusion layer thickness [21] of $\delta = \sqrt{\frac{DRT}{\nu F}} = \sqrt{\frac{10^{-13}\times 8.31\times 293}{0.016\times 96487}} = 0.4\mu$m (assuming a scan rate of ν=0.016 V s^{-1}). Therefore, the limiting charge in Fig. 5c is substantial and may approach exhaustive oxidation. The data in Fig. 5c, d demonstrate the effect of scan rate on the binding isotherms derived from the voltammograms. Reassuringly, the approximate Langmuirian binding constant, $K=4\times 10^4$ M^{-1}, is independent of the scan rate.

Loss of Z907 at the FTO electrode surface can impede the flow of electrons to and from the TiO_2 via hopping, and this can reduce the peak current for Z907 adsorbed onto TiO_2. When the potential is cycled over a wider potential range, it appears that the remaining oxidised dye at the TiO_2 surface which cannot communicate with the substrate by electron hopping can be reduced at a more negative potential due to the onset of bulk conduction due to electron injection into the TiO_2 film [12]. Figure 5b shows a new peak response at −0.5 V versus Ag/AgCl (3 M KCl) which has been attributed to a direct Ru(III/II) reduction for immobilised Z907 via electron conduction through TiO_2 [12]. In spite of this reduction, the voltammetric response at more positive potentials for the immobilised Z907 dye continues to decay and this can primarily be ascribed to the chemical degradation of the Z907 dye at the FTO electrode surface. Interestingly, the peak current for the cathodic response at −0.5 V versus Ag/AgCl (3 M KCl) remains

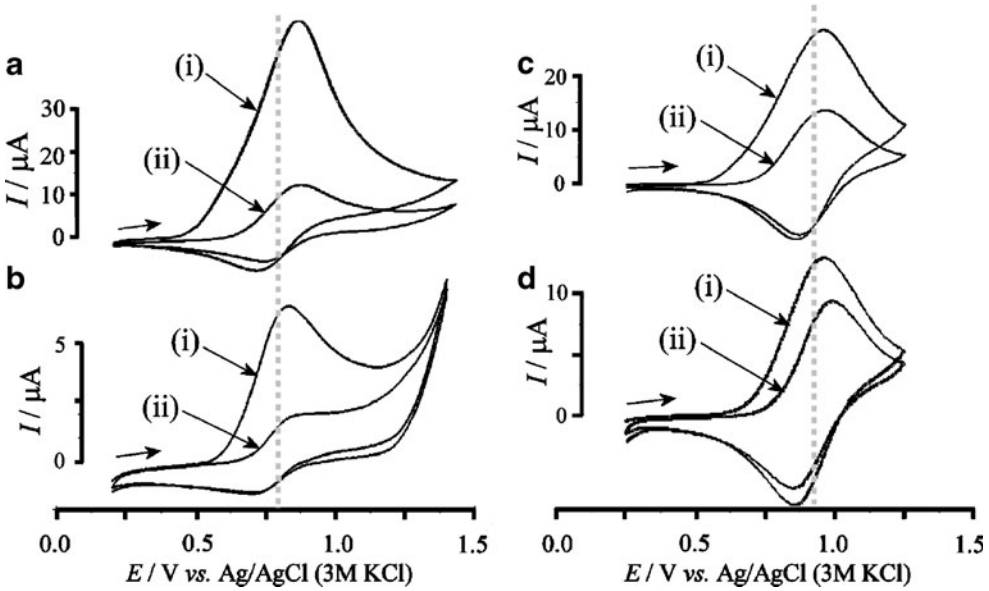

Fig. 6 **a** Cyclic voltammograms (scan rate 16 mV s^{-1}, (*i*) first and (*ii*) second potential cycle) for the oxidation and back reduction of Z907 adsorbed onto a FTO–TiO_2 film electrode (16 h in 10^{-4} M dye solution) immersed in acetonitrile/0.1 M NBu_4PF_6. Electrode area was 9 mm^2. **b** As above showing (*i*) potential cycle 3 and (*ii*) potential cycle 4 recorded after a delay of 10 min. Electrode area was 9 mm^2. **c** Cyclic voltammograms (scan rate 16 mV s^{-1}, (*i*) first and (*ii*) second potential cycle) for the oxidation and back reduction of Z907 adsorbed onto a FTO–TiO_2 film electrode (16 h in 0.5×10^{-3} M dye solution) immersed in acetonitrile/0.1 M NBu_4PF_6. Electrode area was 9 mm^2. **d** As above showing (*i*) potential cycle 3 and (*ii*) potential cycle 4 recorded after a delay of 10 min. Electrode area was 9 mm^2

almost constant which could be interpreted as an insignificant degradation of Z907 on the TiO_2 surface.

The loss of the oxidation response for Z907 adsorbed onto FTO–TiO_2 is shown in Fig. 6. Consecutive cyclic voltammograms at slower scan rate clearly demonstrate the loss of oxidation response (in part due to loss of electron hopping conductivity at the FTO electrode surface and in part due to Ru(III) centres in the TiO_2 which in electron hopping communication with the substrate). When changing the conditions for the Z907 adsorption procedure, again a marked change in the behaviour is observed. The decay of the oxidation response appears much slower when a 16-h deposition and equilibration time in 0.5×10^{-3} M Z907 bath were employed (see Fig. 6c, d). The rate of decay of the voltammetric response for the Ru(III/II) redox process on FTO and on FTO–TiO_2 are very similar which suggests that chemical degradation occurs rather than simple desorption. In the latter case the availability of more weakly bound Z907 from the TiO_2 surface should suppress the loss. This is not observed.

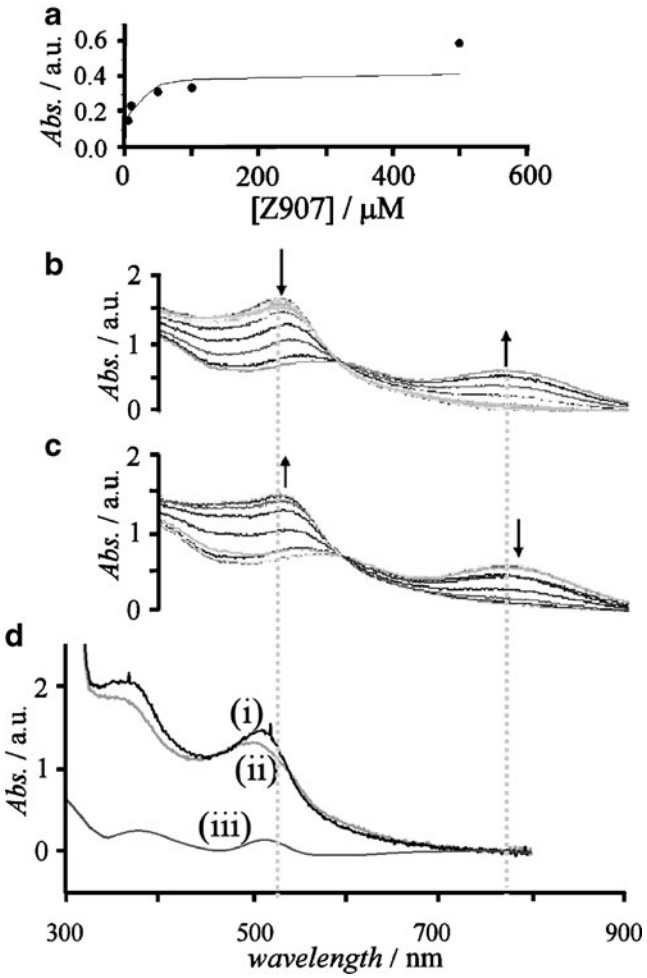

Fig. 7 **a** Plot of absorbance for Z907 on FTO–TiO_2 (at 510 nm) versus Z907 concentration during adsorption onto FTO–TiO_2 film electrodes (16 h in dye solution). The *line* corresponds to a Langmuirian binding constant $K=4\times10^4$ M^{-1}. **b** UV-Vis spectroelectrochemical data (potential range from 0.3 to 1.1 V, stepped by 50 mV every 5 s) for the oxidation of Z907 adsorbed onto a FTO–TiO_2 film electrodes (16 h in 0.5×10^{-3} M dye solution) immersed in acetonitrile/0.1 M NBu_4PF_6. **c** As before but for the reduction of Z907 (potential range from 1.1 to 0.3 V, stepped by −50 mV every 5 s). **d** UV/Vis spectra for Z907 desorbed from a FTO–TiO_2 electrode into a solution of 0.1 M NaOH in aqueous ethanol (50:50). (*i*) Z907 on FTO–TiO_2 (16 h in 10^{-4} M dye solution), (*ii*) Z907 on FTO–TiO_2 electrode after running a 20-cyclic voltammogramme (10 mV s^{-1}) and (*iii*) difference spectrum

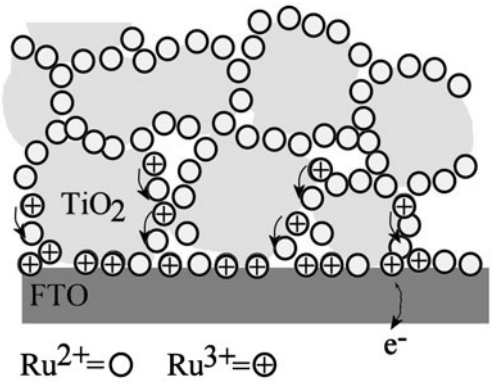

Fig. 8 Schematic representation of the electron hopping mechanism responsible for the Z907 surface electrochemistry on FTO–TiO_2 film electrodes

Spectroelectrochemistry of cis-RuLL'$(SCN)_2$ with L=4,4′-dicarboxylic acid-2,2′-bipyridine and L'=4,4′-dinonyl-2,2′-bipyridine (Z907) at FTO–TiO_2 thin film electrode surfaces

Further insight into the electrochemical and chemical processes for Z907 dye immobilised onto a FTO–TiO_2 film electrode was obtained by spectroelectrochemistry. First, the uptake of Z907 dye into the TiO_2 film was studied by UV/Vis absorption. The resulting coloured FTO–TiO_2 were immersed in aqueous/ethanolic (50:50) 0.1 M NaOH to desorb the Z907. The UV/Vis spectra of the solution after desorption were used to determine the absolute amount of adsorbed Z907. Figure 7a shows that again approximate Langmuirian characteristics are observed with a binding constant of ca. $K=4\times10^4$ M^{-1} in agreement with data obtained by voltammetry (vide supra).

The Z907 dye adsorbed onto TiO_2 shows an absorption maximum at ca. 520 nm (see Fig. 7b). When the applied potential is made more positive than the Ru(III/II) potential, this absorption peak shifts to longer wavelengths and decreases in strength. Simultaneously a new absorption appears at 780 nm, which is a characteristic of the oxidised Z907 Ru(III) system [12]. In the case of a freshly prepared electrode, this process is almost fully reversible as reported in the literature [12]. Figure 7c shows the return of the absorption peak at 520 nm when the potential is cycled

back to 0.3 V versus Ag/AgCl(3 M KCl). When multiple slow scan rate potential cycles are carried out corresponding to exhaustive oxidation conditions the visual appearance of the Z907 modified FT–TiO_2 electrode does not change significantly, but the voltammetric response is diminished as discussed in the previous section. Subsequent desorption of the Z907 dye (after exhaustive potential cycling) into aqueous/ethanolic (50:50) 0.1 M NaOH followed by UV/Vis spectroscopy suggests that only minor chemical changes have occurred (see Fig. 7d). It seems therefore likely that the chemical degradation of Z907 occurs predominantly at the FTO electrode surface and only to an insignificant extent on the TiO_2 surface. The stronger binding of Z907 onto FTO (compared to TiO_2) is likely to result in less mobility, less ordering and a higher strain on the molecules all of which may contribute to the degradation of $Z907^+$. From the UV/Vis data in Fig. 7d the "molecular footprint" for Z907 on TiO_2 can be estimated as 2 nm^2 (assuming 9 nm diameter particles) in excellent agreement with a densely packed surface (vide supra).

Changes observed in voltammetric responses for the Ru (III/II) system are dominated by the electron hopping process directly at the FTO electrode surface (see Fig. 8). Degradation of Z907 at the FTO electrode surface causes a lower rate of hopping conduction and this suppresses the Ru(III/II) surface redox process.

Summary

It has been demonstrated that for the Z907 dye system Ru (III/II) direct redox chemistry can be observed on FTO and on FTO–TiO_2 electrode surfaces. The binding constant for Z907 on FTO is significantly higher compared to that on TiO_2 although the molecular "footprints" for monolayer adsorption are very similar. A fraction of Z907 adsorbed onto FTO undergoes a slow EC-type chemical degradation after oxidation. The dye adsorption conditions allow this fraction to be somewhat reduced. No significant degradation of oxidised Z907 occurs on TiO_2.

The Z907 degradation at the FTO electrode surface could have a small beneficial effect on the operation of solar cells due to a reduced rate of recombination processes (of Ru(III) and electrons) [13] at this interface. However, the absence of chemical Z907 degradation processes on the TiO_2 surface is important for a long operational lifetime under solar cell operation conditions. Further studies of the effects of (a) the solvent environment, (b) other substrates and (c) temperature on the chemical Z907 degradation process will be required and the nature of the degradation product needs to be identified.

Acknowledgments A.F. thanks EPSRC for studentship. We thank the EPSRC Supergen programme for the funding.

References

1. O'Regan B, Grätzel M (1991) Nature 353:737
2. Grätzel M (2001) Nature 414:338
3. Grätzel M (2003) J Photochem Photobiol C 4:145
4. Peter LM (2007) Phys Chem Chem Phys 9:2630
5. Kalyanasundaram K, Grätzel M (1998) Coord Chem Rev 177:347
6. Nazeeruddin MK, Kay A, Rodicio I, Humphry-Baker R, Muller E, Liska P, Vlachopoulos N, Grätzel M (1993) J Am Chem Soc 115:6382
7. Nazeeruddin MK, Zakeeruddin SM, Humphry-Baker R, Jirousek M, Liska P, Vlachopoulos N, Shklover V, Fischer CH, Grätzel M (1999) Inorg Chem 38:6298
8. Zakeeruddin SM, Nazeeruddin MK, Humphry-Baker R, Pechy P, Quagliotto P, Barolo C, Viscardi G, Grätzel M (2002) Langmuir 18:952
9. Kroon JM, Bakker NJ, Smit HJP, Liska P, Thampi KR, Wang P, Zakeeruddin SM, Grätzel M, Hinsch A, Hore S, Wurfel U, Sastrawan R, Durrant JR, Palomares E, Pettersson H, Gruszecki T, Walter J, Skupien K, Tulloch GE (2007) Prog Photovoltaics 15:1
10. Shklover V, Ovchinnikov YE, Braginsky LS, Zakeeruddin SM, Grätzel M (1998) Chem Mater 10:2533
11. Finnie KS, Bartlett JR, Woolfrey JL (1998) Langmuir 14:2744
12. Wang Q, Zakeeruddin SM, Nazeeruddin MK, Humphry-Baker R, Grätzel M (2006) J Am Chem Soc 128:4446
13. Fattori A, Peter LM, Belding SR, Compton RG, Marken F (2010) J Electroanal Chem 640:61
14. Pearson P, Bond AM, Deacon GB, Forsyth C, Spiccia L (2008) Inorg Chem Acta 361:601
15. Dennany L, O'Reilly EJ, Keyes TE, Forster RJ (2006) Electrochem Commun 8:1588
16. Fillinger A, Parson BA (1999) J Electrochem Soc 146:4559
17. Scholz F (2005) Electroanalytical methods, Springer, p 66
18. Kroon JM, Bakker NJ, Smit HJP, Liska P, Thampi KR, Wang P, Zakeeruddin SM, Grätzel M, Hinsch A, Hore S, Wurfel U, Sastrawan R, Durrant JR, Palomares E, Pettersson H, Gruszecki T, Walter J, Skupien K, Tulloch GE (2007) Prog Photovoltaics, Res Appl 15:1
19. Bard AJ, Faulkner LR (2001) Electrochemical Methods. J. Wiley, New York, p 457, BF
20. Wolfbauer G, Bond AM, MacFarlane DR (1999) Inorg Chem 38:3836
21. Scholz F (2005) Electroanalytical methods, Springer p 55